


Research Article

Analytical Solution of Concentrated Mixtures of Hydrogen Sulfide and Methanol in Steady State in Biofilm Model

A. Uma¹, R. Raja^{2,3}, R. Swaminathan^{1*}

¹PG & Research Department of Mathematics, Vidhyaa Giri College of Arts and Science (Affiliated to Alagappa University), Pudukkottai, TamilNadu, India

²Ramanujan Center for Higher Mathematics, Alagappa University, Karaikudi, India

³Department of Computer Science and Mathematics, Lebanese American University, Beirut, Lebanon
E-mail: swaminathanmath@gmail.com

Received: 1 February 2024; **Revised:** 19 May 2024; **Accepted:** 13 June 2024

Abstract: The mathematical model of steady-state biofiltration of hydrogen sulfide and methanol mixtures is explored in this work. The non-linear term associated with monoid kinetics is a part of the system of non-linear reaction-diffusion equations on which this model is built. By applying the Akbari Ganji Method and the Homotopy Perturbation Method to resolve the non-linear equations, an approximate analytical solution of the concentrate mixtures in the biofilm model is obtained. Furthermore, this paper reports numerically by exploiting the Matlab software. By comparing the analytical solution with numerical findings, the accuracy of the method is presented. The new analytical results contribute to optimizing the consistency of this model. These novel approaches produce a compact set of analytical approximations that are straightforward to compute and verify as well.

Keywords: Akbari Ganji Method, biofilm model, Homotopy Perturbation Method, hydrogen sulfide, mathematical modeling, methanol, non-linear equation

MSC: 34A34, 34E05

1. Introduction

Volatile Organic Chemicals released from industrial sources like toluene, hydrogen sulfide, and n-butanol seriously harm human health and the environment [1]. Recent years have seen a major shift in the importance of air purification in environmental research to address issues related to rising air pollution. Critical tasks for sustaining air quality have been highlighted as the control and abatement of harmful odorants. As one of the inorganic components that is produced most frequently, reducing hydrogen sulfide is very crucial. Furthermore, when present in high enough concentrations, it is recognized to be broad-spectrum venom that can target several bodily systems, including the central nervous system.

Many different methods for detoxifying gaseous effluents have been developed. Biological techniques are being used more frequently among these technologies to treat air that has been contaminated by a wide range of contaminants. Undoubtedly, the most widely utilized biological gas treatment technology is biofiltration [2–4]. When compared to other technologies, biofilters have a very low power consumption, which is a big advantage for energy-starved countries.

Copyright ©2024 R. Swaminathan, et al.
DOI: <https://doi.org/10.37256/cm.5320244394>
This is an open-access article distributed under a CC BY license
(Creative Commons Attribution 4.0 International License)
<https://creativecommons.org/licenses/by/4.0/>

Secondly, their capital and operational expenses are quite modest. Sun et al. [5] examined the connection between biomass growth in the reactor and biofilter performance by describing a mathematical model of the dynamic biological and physical processes taking place in a packed trickle-bed air biofilter.

Ottengrál and Vanden Oever were the first to put up a biofiltration model [6]. Several scientists have published the analytical solution for the biofilter particle, which is very beneficial for optimizing the reaction parameter [7–9]. The pH, temperature, moisture content, oxygen content, and nutrients are all favorable conditions that the medium offers the microorganisms. Pollutants move from the vapor phase to the biofilm that forms on the packing particles as the contaminated airstream travels through the filter bed [10].

Complex chemical combinations are typical of the air emissions produced by the forest product sector. The sulfate process (Kraft Process) uses a caustic soda and sodium sulfide solution as the liquor in the pulpwood is cooked to loosen the fibers. This chemical approach is used to produce wood pulp. To make the sulfate process economically viable, salt compounds must be recovered. Hydrogen sulfide and dimethyl sulfide are two reduced Sulphur compounds released during Kraft pulping. Reduced Sulphur Compounds (RSCs) are released from the back liquor oxidation system during the sulfate process [11, 12]. Methanol is the most prevalent Volatile Organic Chemicals (VOC) released for the Kraft process which is emitted from several different effect evaporators.

Sologar et al. [13] used dynamic models to explain how Hydrogen Sulfide and Methanol were eliminated from the biofilter. These mixes can be bio-filtered at modest loading rates and concentrations. The biofiltration of mixtures of hydrogen sulfide and methanol was carried out using two biofilter models, one based on Hirai's [14] reaction-restricted model and the other on Mohseni and Allen's [15] biofilm model.

The ultimate objective of examining the impact of several parameters on the system that governs is still to obtain approximate analytical solutions, despite the existence of numerous effective numerical methods for solving nonlinear equations. Sivasankari et al. [7] worked the analytical expression of the concentration of VOC and Oxygen in the biofiltration model employing the Adomian decomposition Method. Meena et al. [8] derived the analytical formulation of concentration profiles of Methanol and pinene in biofilm and air film phases. Sivasundari et al. [9] examined the transport and kinetics in biofiltration membranes using the Taylor series method and the Akbari Ganji Method.

We believe that our work is the first to present an analytical solution of concentrated combinations of hydrogen sulfide and methanol as representing RSC and VOC respectively. This work aims to present an approximate analytical solution for the aforementioned concentrations using Homotopy Perturbation Method (HPM) and Akbari Ganji Method (AGM). Following that, the issue is then numerically stimulated using a Matlab program. In addition, the solution is illustrated graphically.

2. Mathematical formulation

A mathematical model was used to examine the biofilter's performance in reducing the concentrations of hydrogen sulfide and methanol. Moshini et al. [15] describes the VOC mixed biofiltration model takes into consideration the mass transfer and reaction rate mechanisms in the biofilter and was enhanced to handle above said substances. Two modeling strategies that took into consideration the mass transfer and reaction rate mechanisms in biofilters as well as the sulfide were assessed. It was expected in both scenarios that the liquid trickling solution would have very little effect on mass transfer and reaction rates.

The main objective is to detect the interaction between the two groups of substances namely, hydrogen sulfide, a typical RSC, and Methanol, a representative VOC by biofilter air pollutants containing above said chemicals. Also, determine if the co-treatment is feasible. The presumptions underpin the model, Standardized establishment of biofilm across the wrapping medium, plug flow execution with no rotation fluctuation, monod kinetics, and the existence of all growth aspects besides the substrates that are being evaluated in overabundance. The following set of nonlinear differential equations expresses the steady-state elimination of MeOH in the biofilm [13].

$$\mathcal{D}_{H_2S} X''(x) = a \cdot \frac{A_{H_2S}}{B_{H_2S}} \cdot \frac{\delta X}{\Delta_{H_2S} + X} \quad (1)$$

$$\mathcal{D}_{MeOH} Y''(x) = b \cdot \frac{A_{MeOH}}{B_{MeOH}} \cdot \frac{\delta Y}{\Delta_{MeOH} + Y} \quad (2)$$

Where \mathcal{D}_{H_2S} : Diffusion coefficient of hydrogen sulfide; \mathcal{D}_{MeOH} : Diffusion coefficient of Methanol; X : Concentration of hydrogen sulfide; Y : Concentration of Methanol; x : Dimension across the biofilm; A : Biofilm density; B : Biofilm yield coefficient; δ : Maximum growth rate; Δ : Monod constant.

For the equations (1) and (2), the boundary conditions are stated as

$$\text{At } x = 0, X = \frac{C_{H_2S}}{c_{H_2S}} \text{ and } Y = \frac{C_{MeOH}}{c_{MeOH}}.$$

$$\text{At } x = \mu_{H_2S}, X'(x) = 0.$$

$$\text{At } x = \mu_{MeOH}, Y'(x) = 0.$$

Where c is an air-water partition coefficient and is a biofilm thickness.

Non-Dimensional Form

By specifying the subsequent non-dimensional variables, (1) and (2) are made to be dimensionless.

$$\text{Consider } \tilde{X} = \frac{X}{X_i}; \psi_1 = \frac{X_i}{\Delta_{H_2S}}; \varepsilon_1 = \frac{A \delta_{H_2S}}{B_{H_2S}} \cdot \frac{\mu^2}{\mathcal{D}_{H_2S} \Delta_{H_2S}}; \tilde{x} = \frac{x}{\delta}; \tilde{Y} = \frac{Y}{Y_i}; \psi_2 = \frac{Y_i}{\Delta_{MeOH}}; \varepsilon_2 = \frac{A \delta_{MeOH}}{B_{MeOH}} \cdot \frac{\mu_2}{\mathcal{D}_{MeOH} \Delta_{MeOH}}.$$

Where \tilde{X} and \tilde{Y} are the dimensionless concentration of hydrogen sulfide and methanol, \tilde{x} is the dimensionless distance in biofilm and $\varepsilon_1, \varepsilon_2, \psi_1, \psi_2$ are dimensionless diffusion parameters.

Equations (1) and (2) can be written as the dimensionless form shown below by using the above defined non-dimensional parameters.

$$\tilde{X}''(\tilde{x}) = a \varepsilon_1 \left[\frac{\tilde{X}}{1 + \psi_1 \tilde{X}} \right] \quad (3)$$

$$\tilde{Y}''(\tilde{x}) = b \varepsilon_2 \left[\frac{\tilde{Y}}{1 + \psi_2 \tilde{Y}} \right] \quad (4)$$

With the boundary conditions

$$\tilde{X} = \tilde{Y} = 1, \text{ when } \tilde{x} = 0 \quad (5)$$

$$\tilde{X}' = \tilde{Y}' = 0, \text{ when } \tilde{x} = 1 \quad (6)$$

3. Analytical solution of concentrated mixtures of hydrogen sulfide and methanol in biofilm at steady state

Many writers have focused on researching the solution of nonlinear equations during the past few decades using a variety of techniques, including the Homotopy Perturbation Method [16–19], Taylor Series Method [20–22], Akbari Ganji Method [23–30], Variational Iteration Method [31, 32]. The accuracy of the Akbari Ganji Method and the

Homotopy Perturbation Method for solving nonlinear models have been demonstrated in a variety of scientific and technical disciplines in recent times.

3.1 Akbari-Ganji Method

AGM is one of the effective algebraic strategies that produces an approximate semi-analytic solution of nonlinear differential equations. This approach offers convergent series-based solutions without the need for linearization. The main positive aspect of this approach over other analytical techniques is that it reduces the intrinsic complexity of the solution to the nonlinear differential equations. More AGM applications can be expressed in [23–30].

By AGM, the trial solutions of (3) and (4) are taken as,

$$\tilde{X}(\tilde{x}) = \pi_X \cosh(m\tilde{x}) + \tau_X \sinh(m\tilde{x}) \quad (7)$$

$$\tilde{Y}(\tilde{x}) = \pi_Y \cosh(n\tilde{x}) + \tau_Y \sinh(n\tilde{x}) \quad (8)$$

Where π_X , π_Y , τ_X , τ_Y , m and n are fixed values.

According to the boundary conditions (5) and (6),

$$\tilde{X}(0) = \pi_X \cosh(0) + \tau_X \sinh(0), \text{ at } \tilde{x} = 0$$

$$\therefore \pi_X = 1$$

$$\tilde{Y}(0) = \pi_Y \cosh(0) + \tau_Y \sinh(0), \text{ at } \tilde{x} = 0$$

$$\therefore \pi_Y = 1$$

From (7),

$$\tilde{X}'(\tilde{x}) = m[\tau_X \sinh(m\tilde{x}) + \pi_X \cosh(m\tilde{x})] \quad (9)$$

From (8),

$$\tilde{Y}'(\tilde{x}) = n[\tau_Y \sinh(n\tilde{x}) + \pi_Y \cosh(n\tilde{x})] \quad (10)$$

At $\tilde{x} = 1$ in (9)

$$\begin{aligned}\tilde{X}'(1) &= m[\tau_X \sinh(m) + \tau_X \cosh(m)] \\ \Rightarrow \sinh(m) + \tau_X \cosh(m) &= 0 \\ \Rightarrow \tau_X &= -\tanh(m)\end{aligned}\tag{11}$$

Similarly,

$$\tau_Y = -\tanh(n)\tag{12}$$

Substitute (11) and (12) in (9) and (10) respectively,

$$\tilde{X}'(\tilde{x}) = \cosh(m\tilde{x}) - \tanh(m)\sinh(m\tilde{x})\tag{13}$$

$$\tilde{Y}'(\tilde{x}) = \cosh(n\tilde{x}) - \tanh(n)\sinh(n\tilde{x})\tag{14}$$

Differentiate (13) and (14), we get

$$\tilde{X}''(\tilde{x}) = m^2[\cosh(m\tilde{x}) - \tanh(m)\sinh(m\tilde{x})]\tag{15}$$

$$\tilde{Y}''(\tilde{x}) = n^2[\cosh(n\tilde{x}) - \tanh(n)\sinh(n\tilde{x})]\tag{16}$$

Then (3) becomes,

$$m^2[\cosh(m\tilde{x}) - \tanh(m)\sinh(m\tilde{x})] = a\varepsilon_1 \left[\frac{\cosh(m\tilde{x}) - \tanh(m)\sinh(m\tilde{x})}{1 + \psi_1[\cosh(m\tilde{x}) - \tanh(m)\sinh(m\tilde{x})]} \right]$$

$$\text{At } \tilde{x} = 0, m^2 = \frac{a\varepsilon_1}{1 + \psi_1}.$$

$$\text{Therefore, } m = \left(\frac{a\varepsilon_1}{1 + \psi_1} \right)^{\frac{1}{2}}.$$

$$\text{Similarly, } n = \left(\frac{b\varepsilon_2}{1 + \psi_2} \right)^{\frac{1}{2}}.$$

$$\tilde{X}(\tilde{x}) = \cosh\left(\left(\frac{a\varepsilon_1}{1+\psi_1}\right)^{\frac{1}{2}}\tilde{x}\right) - \tanh\left(\left(\frac{a\varepsilon_1}{1+\psi_1}\right)^{\frac{1}{2}}\right) \sinh\left(\left(\frac{a\varepsilon_1}{1+\psi_1}\right)^{\frac{1}{2}}\tilde{x}\right)$$

$$\tilde{Y}(\tilde{x}) = \cosh\left(\left(\frac{b\varepsilon_2}{1+\psi_2}\right)^{\frac{1}{2}}\tilde{x}\right) - \tanh\left(\left(\frac{b\varepsilon_2}{1+\psi_2}\right)^{\frac{1}{2}}\right) \sinh\left(\left(\frac{b\varepsilon_2}{1+\psi_2}\right)^{\frac{1}{2}}\tilde{x}\right)$$

∴ the analytical solution of concentration of hydrogen sulfide and Methanol in Biofilm model,

$$\tilde{X}(\tilde{x}) = \frac{\cosh\left(\left(\frac{a\varepsilon_1}{1+\psi_1}\right)^{\frac{1}{2}}(\tilde{x}-1)\right)}{\cosh\left(\frac{a\varepsilon_1}{1+\psi_1}\right)^{\frac{1}{2}}} \quad (17)$$

$$\tilde{Y}(\tilde{x}) = \frac{\cosh\left(\left(\frac{b\varepsilon_2}{1+\psi_2}\right)^{\frac{1}{2}}(\tilde{x}-1)\right)}{\cosh\left(\frac{b\varepsilon_2}{1+\psi_2}\right)^{\frac{1}{2}}} \quad (18)$$

3.2 Homotopy Perturbation Method

The homotopy and perturbation methods are combined to form HPM. The author He has introduced this method in 1998 [33–35]. Comparing the other algebraic approaches, it is an efficient technique for solving nonlinear problems with no need for a linearization process. HPM produces a series solution through successive iterations, where each term refines the preceding approximations, and by managing the convergence of this series, HPM furnishes an approximate analytical solution. Nowadays, HPM applications in nonlinear fields of problems have been developed by more scientists and engineers [16–19].

The construction of homotopy for Equation (1) can be written as,

$$(1-p)\left[\tilde{X}''(\tilde{x}) - a\varepsilon_1\left(\frac{\tilde{X}}{1+\psi_1\tilde{X}(0)}\right)\right] + p[(1+\psi_1\tilde{X})\tilde{X}''(\tilde{x}) - a\varepsilon_1\tilde{X}] = 0 \quad (19)$$

Equation (1) has a analytical solution as,

$$\tilde{X} = \tilde{X}_0 + \tilde{X}_1p + \tilde{X}_2p^2 + \dots \quad (20)$$

Substituting (20) in (19)

$$\begin{aligned}
& (1-p)[\tilde{X}_0''(\tilde{x}) + p\tilde{X}_1''(\tilde{x}) + p^2\tilde{X}_2''(\tilde{x}) + \dots] \\
& + p[(\tilde{X}_0''(\tilde{x}) + p\tilde{X}_1''(\tilde{x}) + p^2\tilde{X}_2''(\tilde{x}) + \dots) \\
& + \psi_1(\tilde{X}_0(\tilde{x}) + p\tilde{X}_1(\tilde{x}) + p^2\tilde{X}_2(\tilde{x}) + \dots) \\
& \times (\tilde{X}_0''(\tilde{x}) + p\tilde{X}_1''(\tilde{x}) + p^2\tilde{X}_2''(\tilde{x}) + \dots) - a\varepsilon_1(\tilde{X}_0(\tilde{x}) + p\tilde{X}_1(\tilde{x}) + p^2\tilde{X}_2(\tilde{x}) + \dots)] = 0
\end{aligned} \tag{21}$$

After solving the equation (21), we get

$$\tilde{X}_0''(\tilde{x}) + p\tilde{X}_1''(\tilde{x}) - \left(\frac{a\varepsilon_1}{1+\psi_1}\right)\tilde{X}_0 - p\left(\frac{a\varepsilon_1}{1+\psi_1}\right)\tilde{X}_1 + p\psi_1\tilde{X}_0\tilde{X}_0''(\tilde{x}) = 0 \tag{22}$$

When contrasting the coefficients of different powers of p in (22), we get

$$\tilde{X}_0''(\tilde{x}) - \left(\frac{a\varepsilon_1}{1+\psi_1}\right)\tilde{X}_0 = 0 \tag{23}$$

$$\tilde{X}_1''(\tilde{x}) + \psi_1\tilde{X}_0\tilde{X}_0''(\tilde{x}) - \left(\frac{a\varepsilon_1}{1+\psi_1}\right)\tilde{X}_1 = 0 \tag{24}$$

Solving the second order equation (23), we get the result,

$$\tilde{X}_0(\tilde{x}) = \alpha e^{\left(\frac{a\varepsilon_1}{1+\psi_1}\right)^{\frac{1}{2}}x} + \beta e^{-\left(\frac{a\varepsilon_1}{1+\psi_1}\right)^{\frac{1}{2}}x}$$

It can be written as

$$\tilde{X}_0(\tilde{x}) = \cosh\left(\left(\frac{a\varepsilon_1}{1+\psi_1}\right)^{\frac{1}{2}}x\right) + \beta \sinh\left(\left(\frac{a\varepsilon_1}{1+\psi_1}\right)^{\frac{1}{2}}x\right) \tag{25}$$

Using (5) and (6) as boundary conditions, we obtain

$$\alpha = 1 \text{ and } \beta = -\tanh\left(\frac{a\varepsilon_1}{1+\psi_1}\right)^{\frac{1}{2}}$$

Then (25) becomes,

$$\tilde{X}_0(\tilde{x}) = \cosh\left(\left(\frac{a\varepsilon_1}{1+\psi_1}\right)^{\frac{1}{2}} x\right) - \tanh\left(\left(\frac{a\varepsilon_1}{1+\psi_1}\right)^{\frac{1}{2}}\right) \sinh\left(\left(\frac{a\varepsilon_1}{1+\psi_1}\right)^{\frac{1}{2}} x\right) \quad (26)$$

It can be rewritten as,

$$\tilde{X}_0(\tilde{x}) = \frac{\cosh\left(\left(\frac{a\varepsilon_1}{1+\psi_1}\right)^{\frac{1}{2}} (\tilde{x}-1)\right)}{\cosh\left(\left(\frac{a\varepsilon_1}{1+\psi_1}\right)^{\frac{1}{2}}\right)} \quad (27)$$

Similarly solving (24) and again using the boundary conditions (5) and (6), we get

$$\begin{aligned} \tilde{X}_1(\tilde{x}) &= \frac{\psi_1}{2\cosh^2 k} - \frac{\psi_1}{6\cosh^2 k} [\cosh 2k(\tilde{x}-1)] \\ &+ \left[\frac{\psi_1 \cosh 2k}{6\cosh^2 k} - \frac{\psi_1}{2\cosh^2 k} \right] \left[\frac{\cosh k(\tilde{x}-1)}{2\cosh^2 k} \right] \end{aligned} \quad (28)$$

Where $k = \left(\frac{a\varepsilon_1}{1+\psi_1}\right)^{\frac{1}{2}}$.

The analytical solution of concentration of hydrogen sulfide expressed as

$$\tilde{X}(\tilde{x}) = \tilde{X}_0(\tilde{x}) + \tilde{X}_1(\tilde{x})$$

From (27) and (28), we get the result

$$\begin{aligned} \tilde{X}(\tilde{x}) &= \frac{\cosh k(\tilde{x}-1)}{\cosh k} - \frac{\psi_1 \cosh 2k(\tilde{x}-1)}{6\cosh^2 k} + \frac{\psi_1}{2\cosh^2 k} \\ &+ \left[\frac{\psi_1 \cosh 2k}{6\cosh^2 k} - \frac{\psi_1}{2\cosh^2 k} \right] \left[\frac{\cosh k(\tilde{x}-1)}{2\cosh^2 k} \right] \end{aligned} \quad (29)$$

Similarly solving (4) by using HPM, we get the concentration of Methanol which can be written as

$$\begin{aligned} \tilde{Y}(\tilde{x}) &= \frac{\cosh t(\tilde{x}-1)}{\cosh t} - \frac{\psi_2 \cosh 2t(\tilde{x}-1)}{6\cosh^2 t} + \frac{\psi_2}{2\cosh^2 t} \\ &+ \left[\frac{\psi_2 \cosh 2t}{6\cosh^2 t} - \frac{\psi_2}{2\cosh^2 t} \right] \left[\frac{\cosh t(\tilde{x}-1)}{2\cosh^2 t} \right] \end{aligned} \quad (30)$$

where $t = \left(\frac{b\epsilon_2}{1 + \psi_2} \right)^{\frac{1}{2}}$.

4. Numerical simulation

The efficiency of the methods is demonstrated by contrasting the numerical simulation of the equations (3) & (4) with the Analytical findings (17) and (18) derived by the Akbari Ganji Method and equations (29) and (30) by using Homotopy Perturbation Method. Graphical comparisons between our analytical findings and numerical results demonstrate the effectiveness of the current approach. Table 1, 2, 3, 4 compares the computational outcomes with dimensionless concentrations of hydrogen sulfide and Methane in its analytical representation. These tables show that, for different amounts of diffusion and saturation parameters, our new result agrees rather well with the numerical findings. It provides a satisfactory agreement for all parameter settings under comparison. Our results employing AGM and HPM with numerical results have maximum relative error rates of 0.07% and 0.2% respectively. The nature of the relationship will determine the kind of structure of the negotiation aspects. Stated differently, the functional forms of and will depend on whether the relationships are concentration-dependent and chemical, physical, and biological. There were no discernible interaction effects in this case study. Thus, there was no argument for addressing the interaction parameters gestalt.

Table 1. Comparison of analytical results by AGM (17) and by HPM (29) with numerical result (3) of the H₂S concentration for the constant value of ψ_1 and numerous amount ϵ_1

\bar{x}	$a = 1, \psi_1 = 1, \epsilon_1 = 1$					$a = 1, \psi_1 = 1, \epsilon_1 = 0.1$				
	Num	AGM Eqn (17)	Error % of AGM	HSM Eqn (29)	Error % of HSM	Num	AGM Eqn (17)	Error % of AGM	HSM Eqn (29)	Error % of HSM
0.1	0.9562	0.9594	0.0032	1.0721	0.1159	0.9321	0.9338	0.0017	0.9347	0.0026
0.3	0.8834	0.8924	0.009	1.0464	0.163	0.8219	0.8262	0.0043	0.8335	0.0116
0.5	0.8298	0.8433	0.0135	1.0258	0.196	0.7427	0.7489	0.0062	0.7601	0.0174
0.7	0.7948	0.8112	0.0164	1.0114	0.2166	0.6919	0.6987	0.0068	0.7125	0.0206
0.9	0.7778	0.7953	0.0175	1.0039	0.2261	0.6676	0.6741	0.0065	0.6890	0.0214
Average Error %			0.0119		0.1835			0.0051		0.0147

Table 2. Deviation of analytical findings derived using AGM (17) and using HPM (29) with numerical result (3) of the H₂S concentration for different values of ψ_1 and fixed ϵ_1

\bar{x}	$a = 2, \psi_1 = 0.1, \epsilon_1 = 1$					$a = 2, \psi_1 = 5, \epsilon_1 = 1$				
	Num	AGM Eqn (17)	Error % of AGM	HSM Eqn (29)	Error % of HSM	Num	AGM Eqn (17)	Error % of AGM	HSM Eqn (29)	Error % of HSM
0.1	0.9906	0.9908	0.0002	1.2677	0.2771	0.7768	0.8047	0.0279	0.6186	0.1582
0.3	0.9748	0.9754	0.0006	1.2624	0.2876	0.458	0.5276	0.0696	0.4646	0.0066
0.5	0.963	0.9639	0.0009	1.2584	0.2954	0.2680	0.3577	0.0897	0.3449	0.0769
0.7	0.9552	0.9562	0.001	1.2556	0.3004	0.1654	0.2697	0.1043	0.2679	0.1025
0.9	0.9514	0.9524	0.001	1.2542	0.3028	0.12200	0.2166	0.0946	0.2307	0.1087
Average Error %			0.0007		0.2926			0.0772		0.0273

Table 3. Comparison between analytical results of AGM (18) and HPM (30) with numerical result (4) of MeOH concentration for fixed ψ_2 and various amount of ε_2

\bar{x}	$a = 1, \psi_1 = 0.1, \varepsilon_1 = 0.01$					$a = 1, \psi_1 = 0.1, \varepsilon_1 = 1$				
	Num	AGM Eqn (18)	Error % of AGM	HSM Eqn (30)	Error % of HSM	Num	AGM Eqn (18)	Error % of AGM	HSM Eqn (30)	Error % of HSM
0.1	0.9908	0.9909	0.0001	0.9936	0.0028	0.9952	0.9953	0.0001	1.2995	0.3043
0.3	0.9754	0.9757	0.0003	0.9785	0.0031	0.9873	0.9874	0.0001	1.2968	0.3095
0.5	0.964	0.9643	0.0003	0.9672	0.0032	0.9813	0.9816	0.0003	1.2948	0.3135
0.7	0.9565	0.9567	0.0002	0.9597	0.0032	0.9774	0.9777	0.0003	1.2934	0.316
0.9	0.9528	0.9592	0.0064	0.9559	0.0031	0.9755	0.9757	0.0002	1.2928	0.3173
Average Error %			0.0014		0.0031			0.0002		0.3121

Table 4. Tabulation of analytical solutions for AGM (18) and for HPM (30) with numerical result (4) of MeOH concentration for the different values of ψ_2 and constant value of ε_2

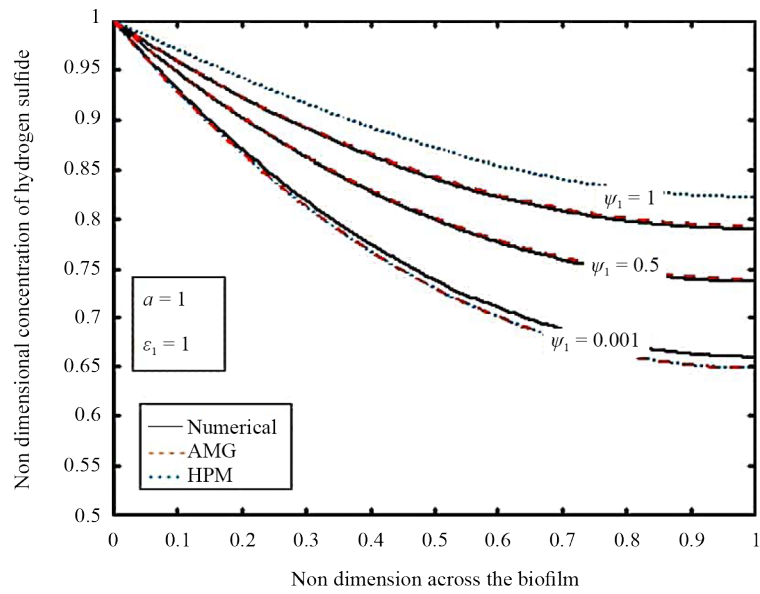
\bar{x}	$a = 2, \psi_1 = 0.01, \varepsilon_1 = 0.1$					$a = 2, \psi_1 = 1, \varepsilon_1 = 0.1$				
	Num	AGM Eqn (18)	Error % of AGM	HSM Eqn (30)	Error % of HSM	Num	AGM Eqn (18)	Error % of AGM	HSM Eqn (30)	Error % of HSM
0.1	0.9983	0.9982	0.0001	1.0305	0.0322	0.8878	0.8909	0.0031	0.8802	0.0076
0.3	0.9954	0.9954	0.0000	1.0278	0.0324	0.7117	0.7198	0.0081	0.7183	0.0066
0.5	0.9932	0.9932	0.0000	1.0258	0.0326	0.5901	0.6013	0.0112	0.6050	0.0149
0.7	0.9917	0.9918	0.0001	1.0244	0.0327	0.5143	0.5269	0.0126	0.5334	0.0191
0.9	0.9910	0.9911	0.0001	1.0237	0.0327	0.4786	0.4909	0.0123	0.4986	0.0200
Average Error %			0.0001		0.0325			0.0095		0.0106

5. Result and discussion

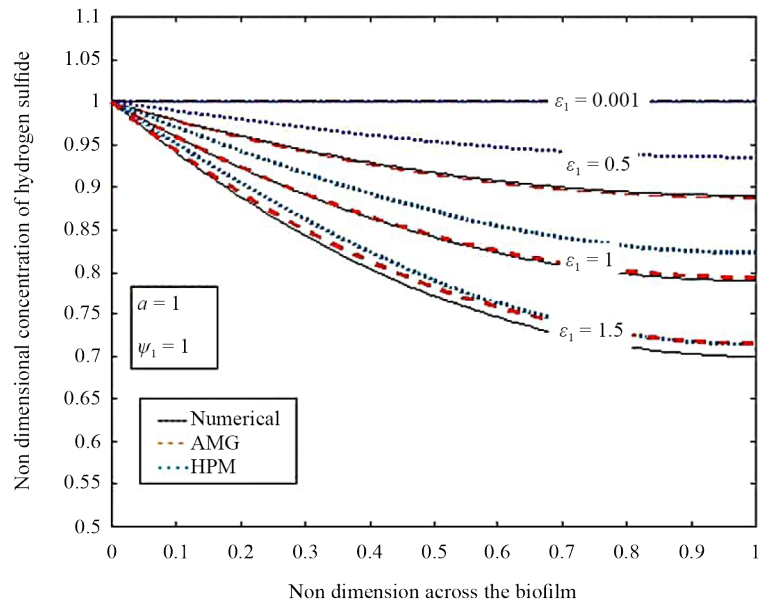
Equations (17)-(18) and (29)-(30) are the analytical solution of the concentrated mixes of Methanol and Hydrogen sulfide solved by using Akbari Ganji Method and Homotopy Perturbation Method respectively. The concentration of these group of substances in the biofilm depends on the reaction rate parameters ε and ψ . We acquired the fluctuation in the non-dimensional parameter ε by changing either the biofilm's thickness or density. Moreover, the parameter ψ is influenced by the half saturation constant and the initial concentration.

Figure 1 shows that the non-dimensional concentration of Hydrogen sulfide in the biofilm versus non dimension across the biofilm for the different values of ψ_1 and for fixed a and ε_1 . As shown in Figure 1(a), for constant values of a and ε , the concentration of Hydrogen sulfide in the biofilm rises as ψ_1 increases. The concentration slowly falls down and reaches the steady state for very small value of reaction rate constant $\psi_1 \leq 1$. That is, the concentration of hydrogen sulfide is directly proportional to the reaction rate constant ψ . As the very large amount of non dimensional position in the biofilm $\bar{x} = 0$, the concentration attains its maximum value and the concentration falls for $\bar{x} \leq 0.5$.

Figure 1(b) evident that the concentration of Hydrogen sulfide rises as ε_1 falls for the fixed value of a and ψ_1 . This graph demonstrates that for each value of ψ_1 and ε_1 that are lower or equal to 1, is approximately comparable to 1. As the concentration of hydrogen sulfide goes down, ε_1 increases. The concentration of reach the lowest value at the large amount of the non dimensional distance in the range of $\bar{x} \leq 0.9$. According to the range $\varepsilon_1 \leq 0.1$, the concentration is uniform. That is the inclined curve turned into the straight line.



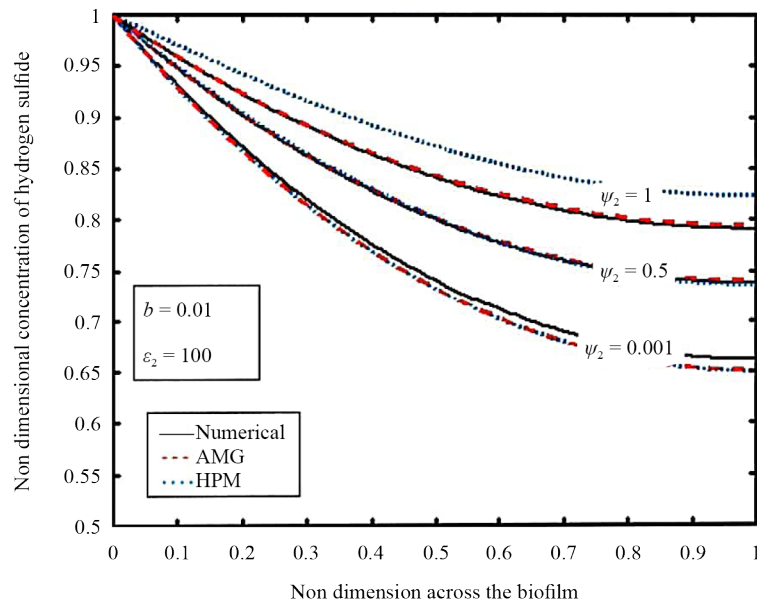
(a)



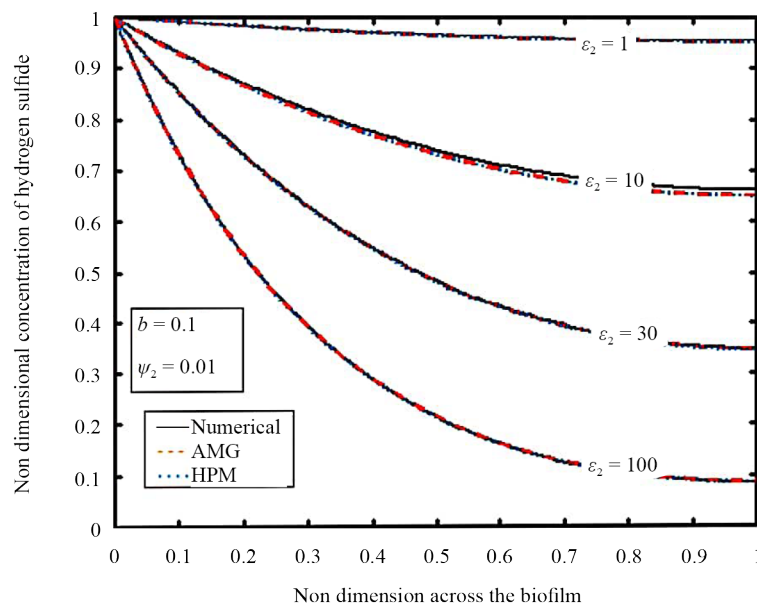
(b)

Figure 1. Comparison of non-dimensional concentration of Hydrogen Sulfide $\bar{X}(\bar{x})$ versus the non dimension across the biofilm whenever (a) for fixed values of a and ϵ_1 as well as different values of ψ_1 (b) for fixed values of a and ψ_1 and various values of ϵ_1

Figure 2 represent that the dimensionless Methanol concentration in the biofilm compared to non dimensional all over the biofilm for the distinct values of ψ_2 and for fixed b , ϵ_2 . Figure 2(a) indicates the Methanol's concentration in the biofilm rises when the range of ψ_2 increases in the case of b and ϵ_2 parameters having fixed values 0.01 and 100 respectively. The concentration of methanol approaches the stable state for the range of position in the biofilm layer $\bar{x} \geq 0.8$. The influence of the parameter ψ_2 which is directionally correlated to the concentration of methanol. The analytical and numerical values are coincide for decreasing values of the reaction rate constant $\xi_{\mathcal{M}}$.



(a)



(b)

Figure 2. Comparison of non-dimensional concentration of Methanol $\tilde{Y}(\tilde{x})$ versus the non dimension across the biofilm whenever (a) for fixed values of b and ϵ_2 and various values of ψ_2 (b) for fixed values of b and ψ_2 and various values of ϵ_2

As seen in Figure 2(b), the concentration of Methanol rises whenever ϵ_2 falls for the fixed value of b and ψ_2 . The concentration of Methanol does not change for small amounts of ϵ_2 . The rate of progress at which the concentration of methanol is extracted from the film drops when the non dimensional parameter for methanol ϵ_2 improves over the biofilm interface. It can be deduced that ϵ_2 is in reverse proportion to methanol concentration, meaning that when the parameter rises, the methanol diffusion coefficient declines or the dimensionless distance grows. The rates at which methanol was removed dependent linearly on concentration. That is, the high concentration attains the stable state.

6. Conclusion

The steady state non-linear reaction diffusion equations in the biofilm model have been solved analytically in this work. The two algebraic methods HPM and AGM are used to provide the analytical solution for the concentrated mixtures of Hydrogen sulfide and Methanol in the biofilm model for various values of parameters. Also the analytical solutions of the concentrated mixtures were compared with numerical simulation results. The parameter's impact on the concentrated mixtures were discussed. These analytical findings allows one to qualitatively evaluate the characteristics of biofilm. These new findings are highly helpful in the design and scalability of biofilters. A wide of multicomponent chemical reactions that utilize different catalyst configurations can be conducted with the presented approximate method stipulated it is sufficient. Concerning other analytical procedures, these two methods are clear-cut, has a straightforward solution, and produces precise results. This technique can solve other boundary value issues in the physical and chemical sciences without difficulty. It is possible to expand the protocol for eliminating hydrogen sulfide and methanol in air stream model and also in non-steady state biofilm model.

Conflict of interest

The authors declare no competing financial interest.

References

- [1] Muñoz R, Daugulis AJ, Hernández M, Quijano G. Recent advances in two-phase partitioning bioreactors for the treatment of volatile organic compounds. *Biotechnology Advances*. 2012; 30(6): 1707-1720.
- [2] Deshusses M. Biological waste air treatment in biofilters. *Current Opinion in Biotechnology*. 1997; 8: 335-339.
- [3] Devinsky J, Deshusses M, Webster T. *Biofiltration for Air Pollution Control*. Boca Raton: CRC Press; 1998.
- [4] Soreanu G, Béland M, Falletta P, Ventresca B, Seto P. Evaluation of different packing media for anoxic H₂S control in biogas. *Environmental Technology*. 2009; 30(2): 1249-1259.
- [5] Sun Y, Quan X, Yang F, Chen J, Lin Q. Effect of organic gas components on biofiltration and microbial density in biofilter. *Chinese Journal of Applied and Environmental Biology*. 2005; 11: 82-85.
- [6] Ottengraf S, Oever AH. Kinetics of organic compound removal from waste gases with a biological filter. *Biotechnology and Bioengineering*. 1984; 25(12): 3089-3102.
- [7] Sivasankari M, Rajendran L. Analytical expressions of concentration of voc and oxygen in steady-state in biofiltration model. *Applied Mathematics*. 2013; 4(2): 314-325.
- [8] Rajendran L. Analytical expression of concentration profiles of methanol and pinene in air stream and bio-film phase. *Journal of Analytical Bioanalytical Techniques*. 2015; 6(1): 1000228.
- [9] Sivasundari S. Transport and kinetics in biofiltration membranes: New analytical expressions for concentration profiles of hydrophilic and hydrophobic VOCs using Taylor's series and Akbari-Ganji methods. *International Journal of Electrochemical Science*. 2022; 17(4): 220447.
- [10] Wani A, Branion R, Lau A. Biofiltration: A promising and cost-effective control technology for Odors, VOCs and air toxics. *Journal of Environmental Science and Health Part A-Toxic/Hazardous Substances Environmental Engineering*. 1997; 32(7): 2027-2055.
- [11] Springer AM. *Industrial Environmental Control*. Norcross, Georgia: Tappi Press; 2000.
- [12] Wani A, Lau A, Branion R. Biofiltration control of pulping odors-hydrogen sulfide: Performance, macrokinetics and coexistence effects of organo-sulfur species. *Journal of Chemical Technology and Biotechnology*. 1999; 74: 9-16.
- [13] Sologar V, Lu Z, Allen D. Biofiltration of concentrated mixtures of hydrogen sulfide and methanol. *Environmental Progress*. 2003; 22(2): 129-136.
- [14] Hirai M, Ohtake M, Shoda M. Removal kinetics of hydrogen sulfide, methanethiol and dimethyl sulfide by peat biofilters. *Journal of Fermentation and Bioengineering*. 1990; 70(5): 334-339.

- [15] Mohseni M, Allen D. Biofiltration of mixtures of hydrophilic and hydrophobic volatile organic compounds. *Chemical Engineering Science*. 2000; 55(9): 1545-1558.
- [16] Swaminathan R, Saravanakumar R, Venugopal K, Rajendran L. Analytical solution of non linear problems in homogeneous reactions occur in the mass-transfer boundary layer: homotopy perturbation method. *International Journal of Electrochemical Science*. 2021; 16(6): 210644.
- [17] Rajendran L, Saranya K, Mohan V, Narayanan K, Swaminathan R. Reaction/diffusion equation with michaelis-menten kinetics in microdisk biosensor: homotopy perturbation method approach. *International Journal of Electrochemical Science*. 2019; 14(4): 3777-3791.
- [18] Swaminathan R, Venugopal K, Rajendran L, Muthuramalingam R, Abukhaled M. Analytical expressions for the concentration and current in the reduction of hydrogen peroxide at a metal-dispersed conducting polymer film. *Química Nova*. 2020; 43(1): 1-8.
- [19] Shunmugham L, Rajendran L. Mathematical modeling of diffusion and kinetics in amperometric immobilized enzyme electrodes. *Electrochimica Acta*. 2010; 55(18): 5230-5238.
- [20] Ramu U, Rajendran L. Taylor's series method for solving the nonlinear reaction-diffusion equation in the electroactive polymer film. *Chemical Physics Letters*. 2020; 754: 137573.
- [21] Ramu U, Rajendran L, Lyons M. Steady-state current in product inhibition kinetics in an amperometric biosensor: adomian decomposition and taylor series method. *Journal of Electroanalytical Chemistry*. 2021; 886(1): 115103.
- [22] Swaminathan R, Devi MC, Rajendran L, Venugopal K. Sensitivity and resistance of amperometric biosensors in substrate inhibition processes. *Journal of Electroanalytical Chemistry*. 2021; 895(3/4): 115527.
- [23] Rajendran L, Swaminathan R, Devi MC. *A Closer Look of Nonlinear Reaction-Diffusion Equations*. New York: Nova Science Publishers, Inc.; 2020.
- [24] Manimegalai B, Lyons M, Rajendran L. A kinetic model for amperometric immobilized enzymes at planar, cylindrical and spherical electrodes: The Akbari-Ganji method. *Journal of Electroanalytical Chemistry*. 2020; 880: 114921.
- [25] Akbari M, Ganji DD, Rostami A, Nimafar M. Solving nonlinear differential equation governing on the rigid beams on viscoelastic foundation by AGM. *Journal of Marine Science and Application*. 2015; 14: 30-38.
- [26] Akbari M, Ganji DD, Nimafar M, Ahmadi A. Significant progress in solution of nonlinear equations at displacement of structure and heat transfer extended surface by new AGM approach. *Frontiers of Mechanical Engineering*. 2014; 9: 390-401.
- [27] Sylvia V, Salomi J, Rajendran L, Lyons M. Theoretical and numerical analysis of nonlinear processes in amperometric enzyme electrodes with cyclic substrate conversion. *Electrochem*. 2022; 3(1): 70-88.
- [28] Reena A, Karpagavalli S, Rajendran L, Manimegalai B, Swaminathan R. Theoretical analysis of putrescine enzymatic biosensor with optical oxygen transducer in sensitive layer using Akbari-Ganji method. *International Journal of Electrochemical Science*. 2023; 18(5): 100113.
- [29] Meresht N, Ganji DD. Solving nonlinear differential equation arising in dynamical systems by AGM. *International Journal of Applied and Computational Mathematics*. 2017; 3: 1507-1523.
- [30] Ranjani K, Swaminathan R, Karpagavalli SG. Mathematical modelling of a mono-enzyme dual amperometric biosensor for enzyme-catalyzed reactions using homotopy analysis and Akbari-Ganji methods. *International Journal of Electrochemical Science*. 2023; 18: 100220.
- [31] Shunmugham L, Rajendran L. Analysis of amperometric enzyme electrodes in the homogeneous mediated mechanism using variational iteration method. *International Journal of Electrochemical Science*. 2010; 5(3): 327-343.
- [32] Rahamathunissa G, Rajendran L. Application of He's variational iteration method in nonlinear boundary value problems in enzyme-substrate reaction diffusion processes: Part 1. The steady-state amperometric response. *Journal of Mathematical Chemistry*. 2008; 44: 849-861.
- [33] He JH. Homotopy perturbation technique. *Computational Methods and Applications of Mechanical Engineering*. 1999; 178: 277-262.
- [34] He JH. A coupling method of a homotopy technique and a perturbation technique for non-linear problems. *International Journal of Non-Linear Mechanics*. 2000; 35(1): 37-43.
- [35] He JH. Asymptotology by homotopy perturbation method. *Applied Mathematics and Computation*. 2004; 156(3): 591-596.